Journal of Applied Sciences

ISSN 1812-5654

science alert

ANSInet
an open access publisher
http://ansinet.com

Journal of Applied Sciences 12 (10): 911-919, 2012
ISSN 1812-5654 / DOI: 10.3923/jas.2012.911.919

Characterization of Electrodeposited Nickel-Al_2O_3 Composite Coatings by Experimental Method and Neural Networks

[1]S. Jeyaraj and [2]K.P. Arulshri
[1]School of Mechanical Engineering, SASTRA University, Thanjavur, 613401, India
[2]Principal, K.P.R. Institute of Engineering and Technology, Coimbatore, 641407, India

Abstract: The development of composite materials and the related design and manufacturing technologies are one of the most important advances in the history of futuristic materials. Composites are multifunctional materials having unprecedented mechanical and physical properties that can be customized to meet the requirements of a particular application. Electrodeposition has been identified to be a technologically feasible and for many applications, economically superior technique for the production of nanocrystalline materials. Composite coating technology has been used extensively in many manufacturing areas. Electroplating, as a methodology is used to produce a thin layer or an additional surface on to a given substrate. Thin layer is produced to modify properties of the substrate such as wear resistance, hardness, lubricity, electrical resistance, etc. Electrodeposited composite coatings which consist of a metal matrix with either a ceramic or cermet particle addition, represent a new development in the field of coating processes. In this study an attempt was made for preparation of Ni-Al_2O_3 composite coatings by adjusting the plating parameters. The results of experimental work such as mass of deposit, volume fraction of Al_2O_3 particles in the deposit and micro hardness of the deposited layer were investigated. A neural network model was trained developed and for the prediction similarities between experimental work and neural network trained results.

Key words: Composite coatings, electordeposition, Ni- Al_2O_3, volume fraction, microhardness, neural networks

INTRODUCTION

Electrodeposition of composite is a technique of co-deposition of fine particles like metallic, non-metallic compounds or polymer particles in the coated layer to enhance material properties such as wear resistance, corrosion resistance, or lubrication. During the plating process, the insoluble particles are in suspended in a conventional plating electrolyte and are co-deposited to the growing metal layer. The second phase material (co-deposition material) can be powder, encapsulated particle or fibre. Existence of the second-phase particles in the deposition which improve properties like micro hardness, yield strength, tensile strength and wear resistance (Ferkel *et al*., 1997).

Tribological coatings improve physical properties such as hardness, lubricity and corrosion resistance, to lower valued substrates that improve overall quality of the base substrate material (Meneve *et al*., 1997). Composite coatings consist of a metal or alloy matrix comprised with a dispersion of second phase particles. The second phase particles are generally oxide or carbide fine particles such as SiC, Al_2O_3, TiO_2, diamond and SiO_2 or solid lubricants like MoS_2, graphite and PTFE to reduce friction or improve wear resistance (Guglielmi, 1972; Roos *et al*., 1990; Hovestad and Janssen, 1995; Benea *et al*., 2001).

Fine particles of oxides, carbides and nitrides having micron and sub-micron sizes can be co-deposited with a variety of metal electroplating metals such as Ni, Co and Cu. In addition, metal-inorganic particles composite can lead to accomplish special properties of coatings such as good hardness and wear corrosion resistance and metal-organic particles can establish new characteristics such as self-lubricating coatings (Kim and Yoo, 1998; Peng *et al*., 1998; Yeh and Wan, 1994; Foster and Cameron, 1976; Pena-Munoz *et al*., 1998).

Hou *et al*. (2002) reported that electrodeposited Ni-SiC composites improve in the wear resistance. Stott and Ashby (1978) investigated that Ni-Al_2O_3 composite coatings have better oxidation resistance than unreinforced nickel in the oxygen enriched atmosphere (Stott and Ashby, 1978). Oxide particles of Al_2O_3 and SiO_2 with fine sizes can be co-deposited along with Ni without difficulty by means of conventional Watts and sulfamate bath (Nwoko and Shreir, 1973).Various investigators have successfully co-deposited second phase particles (like

Corresponding Author: S. Jeyaraj, School of Mechanical Engineering, SASTRA University, Thanjavur, 613401, India
Tel: +91-9524525920

Al_2O_3, SiC, diamond, TiO_2, WC, Cr_3C_2, TiC, etc.) in a variety of metal matrices such as Ni, Cr, Co, Re, etc. (Narayan and Narayana, 1981).

Fabrication of composite coatings by electroplating method is one of the most advanced fabrication technique of Functionally Graded Materials (FGMs). The main advantages of this method over other fabrication techniques are the simplicity to control of process, low initial investment capitals for equipments and possibility to manufacture complicated parts (Guo and Zhang, 1991). In this experimental work, the electrolytic co-deposition of micron and submicron sized Al_2O_3 particles from Nickel Watt's bath solution were carried out. The effect of plating parameters such as current density, temperature of the bath, pH value the bath, concentration of Al_2O_3 particles in electrolyte bath and agitation speed were adjusted for different level of intervals and its effects were analysed. Properties of final deposit such as volume fraction of Al_2O_3 particles, mass of deposit and micro hardness has been studied. Surface morphological studies of Ni- Al_2O_3 coating were carried out with Scanning Electron Microscope (SEM) and metallurgical microscope for identification of behaviour deposited layer. After the experimental investigations a neural network model was developed for the prediction of similarities between the results of experimental work and neural network trainings and simulations. At the end results of neural network model and experimental outcomes such as mass of deposit, volume fraction and micro hardness of coated specimens were compared for similarities.

MATERIALS AND METHODS

The schematic diagram of electroplating setup shown in Fig. 1. Electrodeposition experiments were conducted in a BOROSIL 2000 mL glass container. The plating electrolyte was a watts type nickel bath. Mild steel plate of sized 50.8×25.4×1.8 mm^3 thick was used as a cathode substrate and area of deposition taken as 25.4×25.4 mm^2 (1 $inch^2$). The left behind portions of plating area were masked. A Nickel plate of sized 102×43×5 mm^3 thick was employed as anode in the circuit. Fine sized and decontaminated Al_2O_3 particles (supplied by NICE chemicals (p) Ltd., Cochin, India) with an average size of 5μm and lesser than sized were used as the reinforcement element. A regulated power supply unit made by Spark Tek (0-2 A, 0-30 V, DC supply) was used for the electrodeposition. Temperature of the bath was accurately controlled using Osham temperature controller unit (230 volt, 50 Hz, 30-110°C, AC type). A motorised mechanical stirrer was used to agitate and keep the Al_2O_3 particles in suspension in the electrolyte and whose

Table 1: Process parameters and their levels

Plating parameters	Conditions
Current density	1-4 A dm^{-2}
pH	2.5-4
Temperature	30-60°C
Agitation speed	200-400 rpm
Concentration of the bath	10-30 g L^{-1}

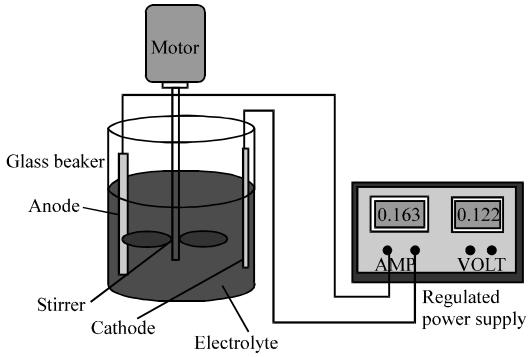

Fig. 1: Experimental setup

rotations were monitored by a digital tachometer. The pH of the solution was monitored by digital pH meter (Made by HANNA Instruments, Mauritius). The pH of bath was adjusted with diluted H_2SO_4 and NaOH solutions depending upon the plating conditions. The plating conditions taken for this experimental test are given in Table 1.

Before plating, each mild steel plate was smoothly polished in dry cloth buffing wheel, degreased with acetone. Initial weight of the each specimen was observed before deposition using electronic weighing machine. Subsequently the specimen was masked and cleaned by anodic and cathodic preparations. In plating bath, the distance between the anode (Ni) and cathode (Mild steel substrate) was maintained constantly for all experiments. Plating time was taken as 60 min in all cases. After co-deposition, the final weights of samples were absorbed. The mass of deposition was measured from the difference of initial and final weights of the specimen.

Surface morphology and distribution of Al_2O_3 particles in the deposit was examined by scanning electron microscope with various magnifications and the volume percentage of embedded alumina particles were determined from micrograph images using METZER-METZ 56 model (Magnification range: 10-2500X) metallurgical microscope. Assessments of micro hardness of the deposits were carried out in VAISESHIKA-Vickers microhardness tester TYPE 7005 with the pay load of 200 g for 15 sec indentation period. The indentation dimensions were examined at 400X magnification and the hardness values were formulated.

After the experimental investigations, a feed forward back propagation neural network model was developed. The neural network model was framed and trained up with experimental parameters and the outcomes of the same. The input layer of network composed with five parameters such as current density, temperature of the bath, pH value the bath, concentration of Al_2O_3 particles in electrolyte bath and agitation speed and target composed with mass of deposit, volume percentage of Al_2O_3 and micro hardness were considered in network training and modelling. In the end, the consequences of experimental and neural networks were compared for the proportion of resemblances.

RESULTS AND DISCUSSION

The experimental results mainly discussed with effect of current density, pH, temperature of the bath, alumina concentration in bath and agitation speed which took part in an important role in the determination of mass of deposit, hardness and volume fraction.

Effect of plating parameters: The effects of selected plating parameters on Ni-Al_2O_3 coating were determined. Figure 2 shows the results of volume percentage of alumina at different current density and pH levels. It was observed that increasing current density produced higher deposition. When current density amplified from 2-3 A dm^{-2}, volume percentage of alumina increased in the deposit. It appeared that the amount of alumina in the nickel matrix increased with current density of 2 A dm^{-2} and reached a maximum about 46.33% with the pH level of 2.5.

From the experimental outcome, the volume fraction of alumina increased with pH value shown in Fig. 3. The greater effect of pH value of bath for better deposition of alumina was positioned between 2.5-3.5. The maximum amount of alumina in deposit, when the pH value was around 2.5 and the least value of alumina deposition (14.31%) at pH 4. It is clarified that the deposition of alumina was reduced with increase in pH.

The volume percentage of alumina incorporated into the nickel matrix was affected by bath temperature as shown in Fig. 4. It appeared that the amount of alumina in the nickel matrix increased with increase in current density and temperature level of 45°C. After this temperature level alumina deposition progressively decreased for all current conditions.

The Fig. 5 corresponds to the effect of concentration of alumina in the bath. The bath concentration was varied from 10-30 g L^{-1} with an interval of 5 g L^{-1}. The highest of alumina deposit was obtained between the bath concentrations of 10-30 g L^{-1}. The mass of deposit was

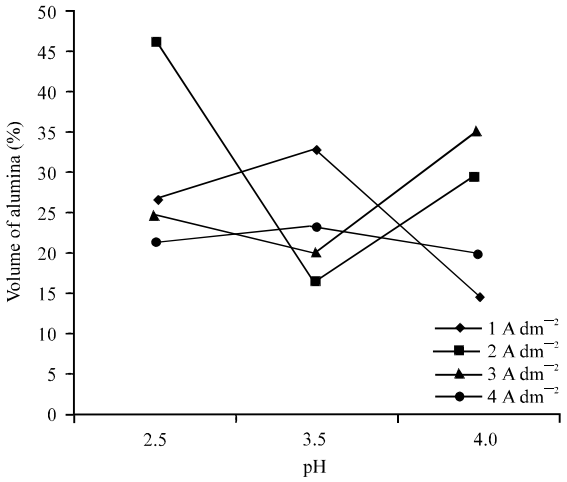

Fig. 3: The relation of pH value of bath with volume of alumina in deposit

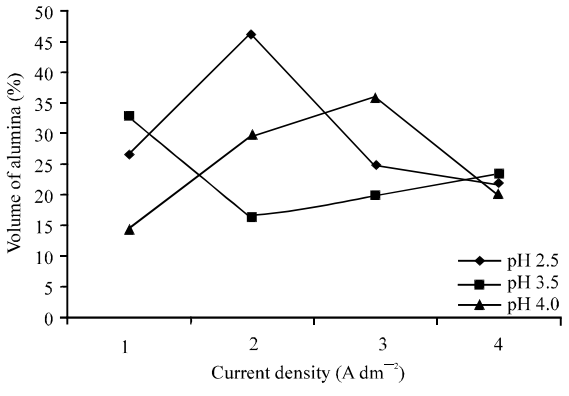

Fig. 2: The relation of current density A dm^{-2} with volume of alumina in deposit

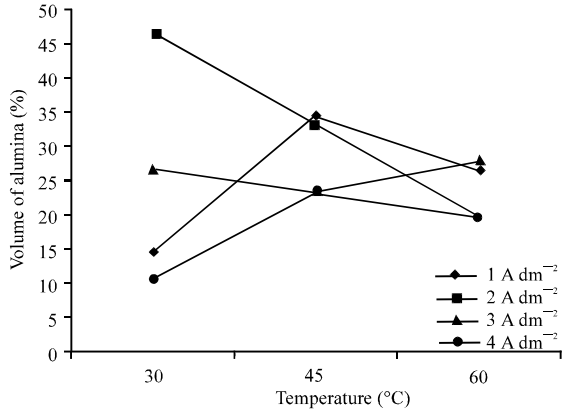

Fig. 4: The relation of temperature with volume of alumina in deposit

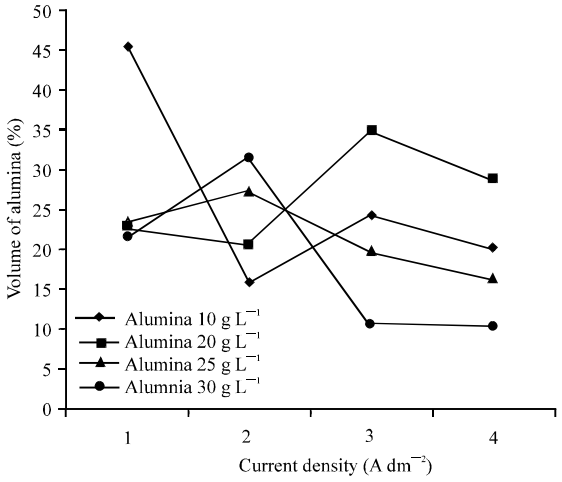

Fig. 5: The relation of bath concentration with volume of alumina in deposit

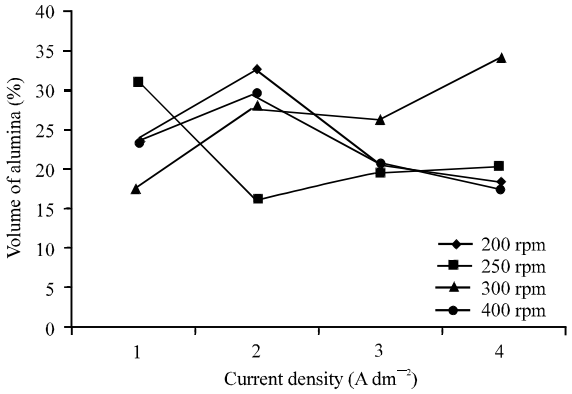

Fig. 6: The relation of agitation speed with volume of alumina in deposit

gradually increased with respect to increase in bath concentration. The deposition rate of alumina was decreased gradually after current density level of 3 A dm^{-2} for all concentration levels.

The purpose of agitation to kept the alumina particles in suspension in the electrolyte. In this experiment the mechanical stirrer was used to keep the particles in suspension in the electrolyte solution by continuous stirring. Figure 6 shows the effect of agitation speed for enhanced deposition of alumina in the deposit. It was observed that highest amount of alumina deposit was obtained between agitation speed levels of 200-300 rpm with current density level of 2 A dm^{-2}.

Effect of current density on mass of deposit: The effect of current density on mass of deposit was shown in Fig. 7. It is observed that increase in current density slightly

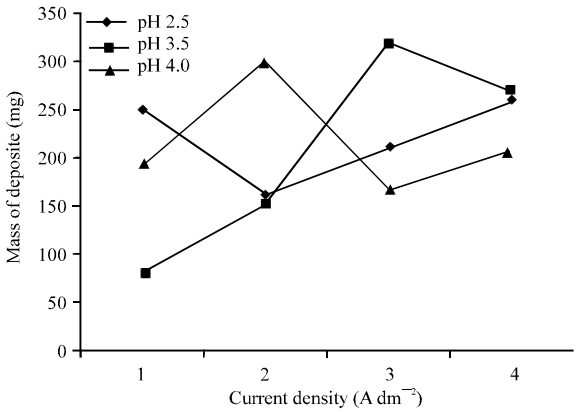

Fig. 7: The relation of current density with mass of deposit

increase in mass of deposit and similar trends observed at all pH levels. At the stage of 3.5 pH and current density 3 A dm^{-2} utmost mass of deposition was found.

Effect of vol.% of alumina on micro hardness: Micro hardness test of the composite coating was carried out in VAISESHIKA-Vickers micro hardness tester TYPE 7005 with the pay load of 200 g for 15 sec indentation period. The indentation in the coated layer was examined at 400X magnification and it was positioned for measurement of indentation diagonal length D. The micro hardness was calculated by the system based on:

$$\text{Micro hardness (Hv)} = \frac{(1.854 \times W)}{(\text{Least count} \times D)^2}$$

Where:

W	=	Load in kg
D	=	Diagonal length in mm
Least count	=	0.000084 mm

The effects of volume fraction of alumina and current density in micro hardness of deposit were shown in Fig. 8. Micro hardness of the specimen was varied with volume of alumina in the matrix. It was examined that the micro hardness of Ni-Al_2O_3 deposit increased with increase in volume percentage of reinforcement particles in the nickel matrix and accomplished highest micro hardness of 405.48 Hv and good hardness values were attained around 30-40% of alumina in the matrix with current density span of 2-4 A dm^{-2}.

Surface morphology of Ni-Al_2O_3 composite coating: The photographic image of specimens after deposition is

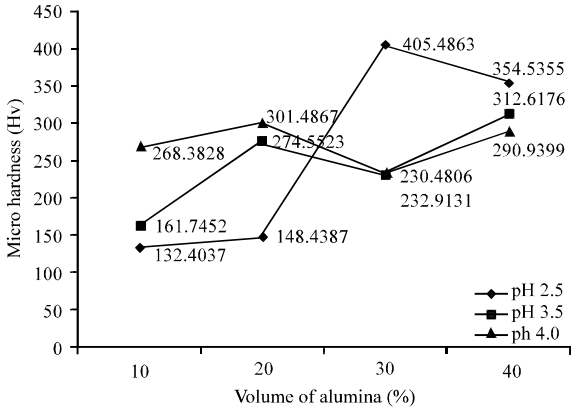

Fig. 8: Effect of vol. fraction of alumina in micro hardness at different pH levels

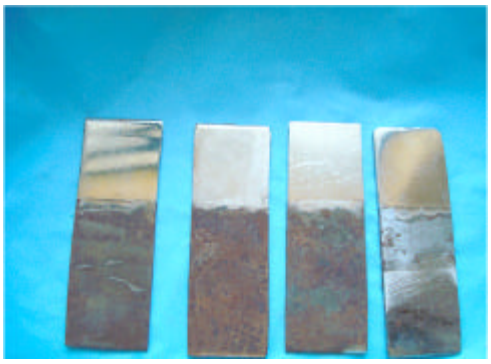

Fig. 9: Snapshot image of specimens after deposition

exposed in Fig. 9. The surface morphologies of Ni- Al_2O_3 composite coating were observed by Scanning Electron Microscope (SEM) revealed in Fig. 10 and 11 with different volume fractions of alumina with 46.33 and 32.76%, respectively. It can be seen that incorporation of Al_2O_3 particles in nickel matrix with the mentioned volume percentages. Also the Fig. 12 illustrates the cross-section microstructure of the deposit containing 46.33% of alumina.

Exploration of experimental works with artificial neural network for the analysis of resemblances: Artificial Neural Network (ANN) techniques are vastly supple modelling equipment with a facility to learn the mapping between input variables and output characteristics (Thillaivanan *et al*., 2010). In this study a feed forward back propagation neural network model was trained and developed using experimental statistics and results. The input parameters current density, temperature, concentration of bath, volume percentage of Al_2O_3, pH of

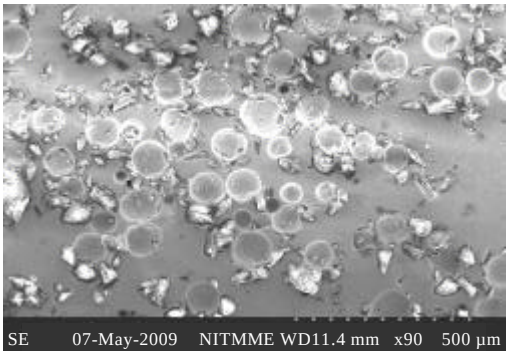

Fig. 10: Microstructure obtained at Current: 2 A dm^{-2}, pH: 3.5, Temperature: 30°C, with 10 g L^{-1} of Al_2O_3 effected with 46.33% of alumina in the nickel matrix

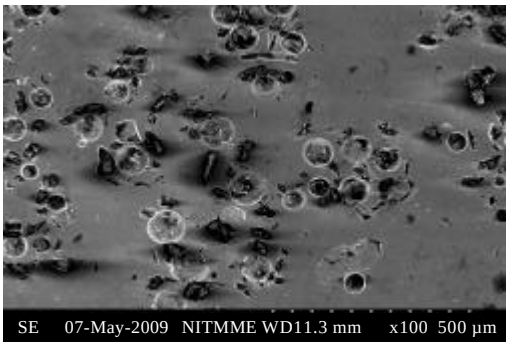

Fig. 11: Microstructure obtained at Current: 2 A dm^{-2}, pH: 3.5, Temperature: 45°C, with 10 g L^{-1} of Al_2O_3 effected with 32.76% of alumina in the nickel matrix

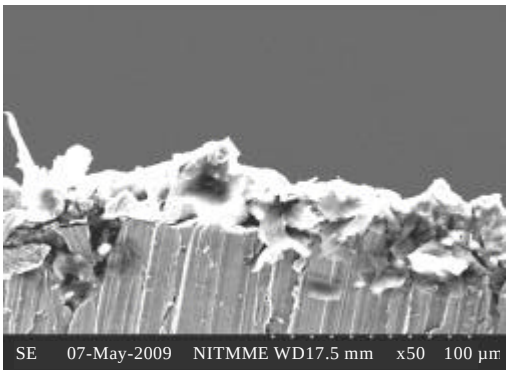

Fig. 12: Cross sectional view of the deposited specimen with 46.33% of alumina

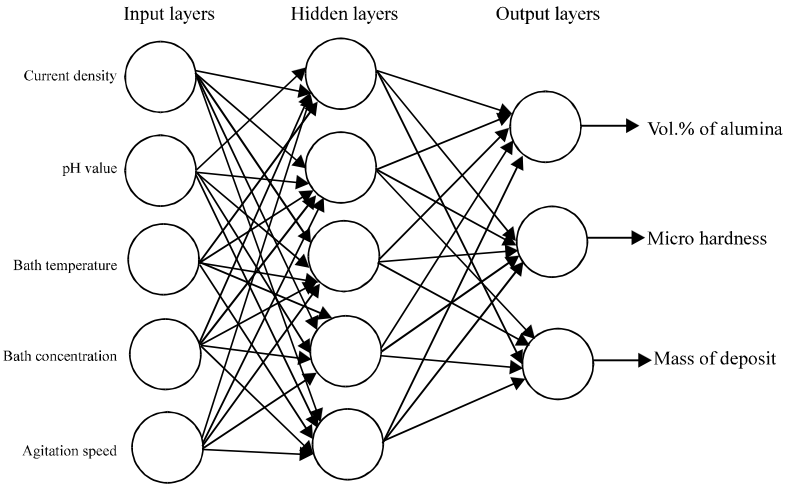

Fig. 13: Neural network structure used for training with 1 input layer, 1 hidden layer with 5 neurons and 1 output layer

the solution and the output constrains such as percentage of Al_2O_3, mass of deposit and micro hardness were taken for network training. The architecture of network model is given in Fig. 13. The network consists of one input layer, one hidden layer with 5 neurons and one output layer which was utilized for training of network.

For uniformed training and analysis, the experimental data sets should be normalized between 0 and 1. The input parameters and the outcomes of the experimental works were normalized. The general method applied for normalization is:

$$Xn = \frac{X - Xmin}{Xmax - Xmin} \quad (1)$$

where, Xn-normalized valve, Xmin and Xmax are the least and highest value in the parameter dataset and the X stands for the value to be normalized. The experimental data sets were normalized and utilized for network training. The Table 2 shows the normalized input parameters used for training and modeling of network.

ANN training algorithm for development of feed forward back propagation network: The normalized experimental input and output parameters were trained with the use of feed forward back propagation module in ANN tool. In the network model, inputs were considered as P and targets were T. The network was created with one hidden layer of five neurons. ANN training response result was mainly based on number of neurons and the epoch values. Initially the network was trained for 5 neurons and 300 epochs. But the test values were not in correlation with validation values for the above neuron and epoch

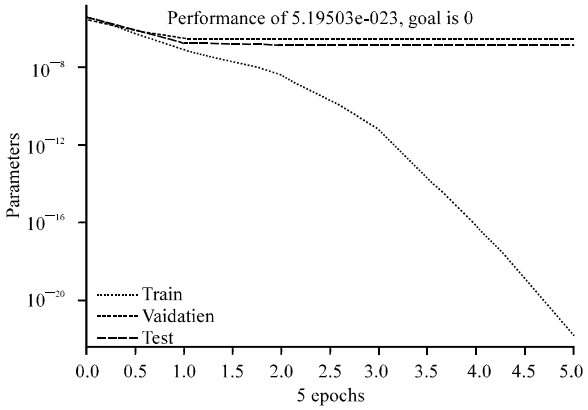

Fig. 14: Training response chart for 38 neurons and 300 epochs which shows closer relation between test values and validation values

setup and testing curve is not linear. So the value of neuron and epoch setup needs to be increased. After the network was trained for 10 neurons and 300 epochs which clearly visualized that the test values were not in mate with the validation values and testing curve was also not linear. So still the neuron size needs to be increased to reach the goal of 0. After a number of iterations with different neuron and epoch setups the network was trained for 38 neurons and 300 epochs. This particular structure offers the output values which are closer to the target set values with very little error. It was clearly visualized that the test values are in near correlated with the validation values. The predicted ANN results were well associated with experimental values shown in training response chart of Fig. 14. Further, increase of neuron

Table 2: Normalized data sets of input parameters for network training

Ex. No.	Current density (A dm^{-2})	pH	Temp. (°C)	Speed rpm	Conc. of bath (g L^{-1})
1	0.12	0.10	0.10	0.14	0.10
2	0.12	0.14	0.10	0.14	0.10
3	0.12	0.14	0.14	0.14	0.10
4	0.14	0.14	0.14	0.14	0.10
5	0.14	0.14	0.18	0.14	0.10
6	0.14	0.16	0.18	0.14	0.10
7	0.16	0.10	0.14	0.18	0.10
8	0.14	0.16	0.10	0.14	0.10
9	0.14	0.16	0.14	0.14	0.10
10	0.12	0.10	0.10	0.14	0.16
11	0.12	0.14	0.10	0.14	0.16
12	0.12	0.14	0.14	0.14	0.16
13	0.14	0.14	0.14	0.14	0.16
14	0.14	0.14	0.18	0.14	0.16
15	0.14	0.16	0.18	0.14	0.16
16	0.14	0.16	0.10	0.18	0.16
17	0.16	0.10	0.14	0.18	0.16
18	0.14	0.16	0.14	0.14	0.16
19	0.12	0.10	0.10	0.14	0.14
20	0.12	0.14	0.10	0.18	0.14
21	0.12	0.14	0.14	0.18	0.14
22	0.14	0.14	0.14	0.18	0.14
23	0.16	0.14	0.14	0.18	0.14
24	0.18	0.14	0.14	0.18	0.14
25	0.12	0.14	0.18	0.18	0.14
26	0.14	0.14	0.18	0.18	0.14
27	0.16	0.14	0.18	0.18	0.14
28	0.18	0.14	0.18	0.18	0.14
29	0.14	0.18	0.10	0.18	0.14
30	0.12	0.14	0.14	0.10	0.14
31	0.14	0.14	0.14	0.10	0.14
32	0.12	0.14	0.18	0.10	0.14
33	0.14	0.14	0.18	0.10	0.14
34	0.16	0.10	0.14	0.12	0.14
35	0.16	0.12	0.14	0.12	0.14
36	0.16	0.14	0.14	0.12	0.14
37	0.16	0.16	0.14	0.12	0.14
38	0.16	0.10	0.18	0.12	0.14
39	0.16	0.12	0.18	0.12	0.14
40	0.16	0.14	0.18	0.12	0.14
41	0.16	0.16	0.18	0.12	0.14
42	0.10	0.14	0.14	0.12	0.18
43	0.12	0.14	0.14	0.12	0.18
44	0.14	0.14	0.14	0.12	0.18
45	0.16	0.14	0.14	0.12	0.18
46	0.10	0.14	0.18	0.12	0.18
47	0.12	0.14	0.18	0.12	0.18
48	0.14	0.14	0.18	0.12	0.18
49	0.16	0.14	0.18	0.12	0.18

size will yield performance value near to the goal of 0 but it requires more number of neurons.

Comparison chart for the resemblance of experimental model and ANN model: After training the target results of the trained network were tabulated with experimental works. The Table 3 shows the end results of experimental work and training results of the network. The linearity between experimental values and neural network results are shown in the statistical plots with its straight line equations and R^2 values. Figure 15 shows the comparison of volume fractions of alumina with experimental and ANN values. The correlation coefficient of this relation obtained was 0.9231. Similarly, Fig. 16 and 17 show the resemblance of experimental model and ANN values for micro hardness and mass of deposits with the correlation coefficients 0.9979 and 0.998, respectively. This statistics clearly states that the experimental values were in good association with the predicted ANN results.

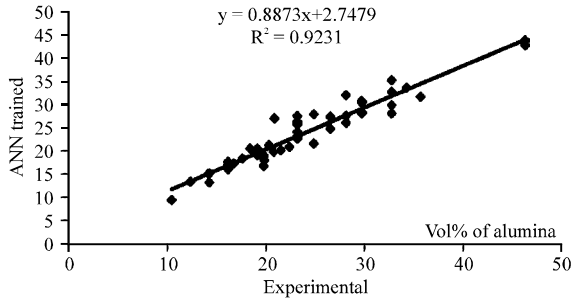

Fig. 15: Evaluation of volume fraction of alumina with experimental and ANN results with the correlation $R^2 = 0.9231$

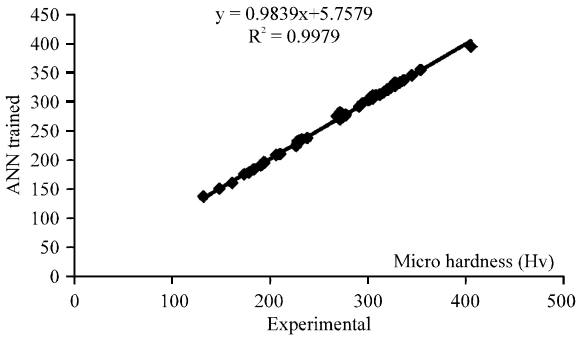

Fig. 16: Evaluation of micro hardness with experimental and ANN results with the correlation $R^2 = 0.9979$

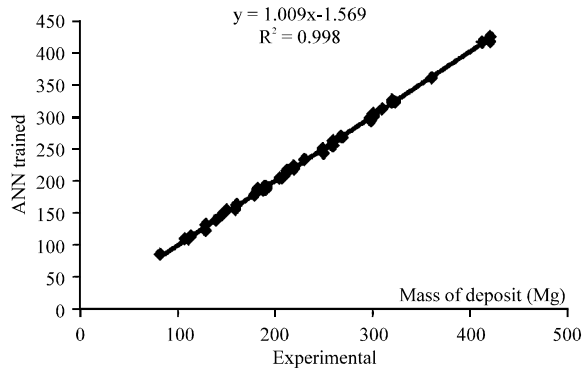

Fig. 17: Evaluation of mass of deposit with Experimental and ANN results with the correlation $R^2 = 0.998$

Table 3: Comparison table for experimental and ANN Training results

Experiment No.	Experimental results			ANN training results		
	Mass of deposit (mg)	Volume of alumina (%)	Micro hardness (Hv)	Mass of deposit (mg)	Volume of alumina (%)	Micro hardness (Hv)
1	115.43	17.65	173.72	114.71	18.55	176.13
2	162.24	46.33	148.44	163.91	43.58	151.66
3	140.89	32.76	178.56	139.80	29.84	179.34
4	213.33	23.23	405.49	216.89	22.79	394.07
5	192.36	28.14	194.35	192.16	27.51	195.54
6	206.05	20.92	328.44	205.52	26.98	327.21
7	260.87	21.53	354.54	262.87	20.40	355.38
8	190.37	14.32	268.38	190.96	13.34	275.34
9	214.42	46.33	305.13	216.60	42.66	310.57
10	109.19	19.88	183.60	110.96	18.22	184.50
11	113.08	19.13	194.35	110.71	19.22	196.63
12	130.27	28.14	328.44	123.81	26.13	330.19
13	210.65	28.14	301.49	209.27	31.99	304.22
14	190.28	34.24	328.44	191.98	33.67	331.06
15	188.82	35.69	232.91	186.86	31.59	235.09
16	208.39	19.82	290.94	205.76	17.01	291.39
17	420.41	16.18	271.44	418.49	16.31	269.70
18	190.24	32.76	320.38	190.92	28.17	321.69
19	130.64	16.24	237.90	132.96	17.29	238.14
20	151.95	14.18	206.06	156.09	15.29	208.99
21	180.05	29.71	271.44	178.95	28.43	281.79
22	259.10	24.91	320.38	256.82	27.93	321.04
23	301.70	23.23	328.44	305.84	25.86	329.76
24	320.77	23.23	345.50	327.44	23.31	345.23
25	160.74	29.71	228.09	156.65	28.02	233.01
26	260.72	20.34	294.39	256.53	21.32	297.49
27	360.96	19.78	316.47	361.92	19.31	316.96
28	420.78	12.41	308.84	426.37	13.64	311.18
29	231.32	24.91	328.44	234.47	21.66	333.29
30	192.21	23.23	190.66	188.29	27.53	192.37
31	250.68	32.76	305.13	244.05	32.64	305.99
32	183.66	20.78	228.09	189.32	20.02	230.00
33	220.20	19.16	277.72	224.78	20.68	276.80
34	310.56	10.46	336.81	313.28	9.79	337.02
35	260.34	26.54	332.59	263.76	24.89	332.64
36	412.41	19.78	323.57	417.40	18.97	324.41
37	298.97	16.78	274.55	294.92	17.46	275.68
38	300.80	29.71	301.49	303.11	30.75	303.00
39	300.73	12.41	277.72	305.23	13.66	278.19
40	270.02	23.23	328.44	269.43	26.37	328.37
41	298.13	14.32	226.44	299.08	15.33	224.32
42	84.16	32.76	161.75	86.75	35.22	162.23
43	146.94	16.17	274.55	147.96	17.90	273.64
44	323.76	18.41	230.48	324.22	20.66	233.65
45	268.52	23.23	312.62	270.49	24.26	312.86
46	250.15	26.54	132.40	251.31	27.37	138.92
47	220.44	19.01	210.20	219.76	20.15	210.31
48	301.55	22.43	228.09	300.97	20.99	229.38
49	320.63	29.71	274.55	323.72	30.46	276.20

CONCLUSIONS

In this research work experimental trials were conducted for different intervals of current densities, pH, concentration of Al_2O_3 in bath, agitation speed, bath temperature. Volume fraction of alumina in the deposit was predicted and fell down between the ranges of 10.45- 46.32%. In order to ascertain the validity of the above experimental, microscopic image analysis was carried out. These results also confirmed the above microscope observation of the Al_2O_3 particles.

The determination of hardness value of deposits was measured from Vickers micro hardness testing machine with the pay load of 200 g and the micro hardness values were placed between 138.92-405.49 Hv. The mass of deposit was determined accurately with the help of electronic balance with the utmost deposition of 420.78 mg. The experimental input parameters and its effects such as mass of deposit, volume fraction and the micro hardness were employed for neural network training and simulation for the achievement of goal.

The experimental effects and the ANN results were compared by the graphical representation for its resemblances. The above neural network simulations were useful for the prediction of mass of deposit, volume fraction of Al_2O_3 and the micro hardness at any set of input parameter setups within the prescribed level. Such predictions will avoid unnecessary conveyance of experiments in future.

REFERENCES

Benea, L., P.L. Bonora, A. Borello and S. Martelli, 2001. Wear corrosion properties of nano-structured SiC-nickel composite coatings obtained by electroplating. Wear, 249: 995-1003.

Ferkel, H., B. Muller and W. Riehemann, 1997. Electrodeposition of particle strengthened nickel films Mater. Sci. Eng. A., 234: 474-476.

Foster, J. and B. Cameron, 1976. Effect of current density and agitation on the formation of electrodeposited composite coatings. Trans. Inst. Met. Finish., 54: 178-183.

Guglielmi, N., 1972. Kinetics of the deposition of inert particles from electrolytic baths. J. Electrochem. Soc., 119: 1009-1012.

Guo, H.T. and S.Y. Zhang, 1991. Composite Coatings. Tianjin University Press, China, Pages: 53.

Hou, K.H., M.D. Ger, L.M. Wang and S.T. Ke, 2002. The wear behaviour of electro-codeposited Ni-SiC composites. Wear, 253: 994-1003.

Hovestad, A. and L.J.J. Janssen, 1995. Electrochemical codeposition of inert particles in a metallic matrix. J. Applied Electrochem., 25: 519-527.

Kim, S.K. and H.J. Yoo, 1998. Formation of bilayer Ni-SiC composite coatings by electrodeposition. Surf. Coatings Technol., 108-109: 564-569.

Meneve, J., K. Vercammen, E. Dekempeneer and J. Smeets, 1997. Thin tribological coatings: Magic or design? Surface Coatings Technol., 94-95: 476-482.

Narayan, R. and B.H. Narayana, 1981. Electrodeposited composite metal coatings. J. Electrochem. Soc., 128: 1704-1708.

Nwoko, V.O. and L.L. Shreir, 1973. Electron micrographic examination of electrodeposited dispersion hardened nickel. J. Appl. Electrochem., 3: 137-141.

Pena-Munoz, E., P. Bercot, A. Grosjean, M. Rezrazi and J. Pagetti, 1998. Electrolytic and electroless coatings of Ni-PTFE composites Study of some characteristics. Surf. Coatings Technol., 107: 85-93.

Peng, X., D.H. Ping, T.F. Li and W.T. Wu, 1998. Oxidation behavior of a Ni-La[sub 2]O [sub 3] codeposited film on nickel. J. Electrochem. Soc., 145: 389-389.

Roos, J.R., J.P. Celis, J. Fransaer and C. Buelens, 1990. The development of composite plating for advanced materials. J. Miner. Met. Mater. Soc., 42: 60-63.

Stott, F.A. and D.J. Ashby, 1978. The oxidation characteristics of electrodeposited nickel composite containing silicon carbide particles at high temperature. Corros. Sci., 18: 183-198.

Thillaivanan, A., P. Asokan, K,N. Srinivasan and R. Saravanan, 2010. Optimization of operating parameters for EDM process based on the Taguchi method and artificial neural network. Int. J. Eng. Sci. Technol., 2: 6880-6888.

Yeh, S.H. and C.C. Wan, 1994. Codeposition of SiC powders with nickel in a Watts bath. J. Applied Electrochem., 24: 993-1000.